Transportation Research Part D 134 (2024) 104338

Contents lists available at ScienceDirect

Transportation Research Part D

journal homepage: www.elsevier.com/locate/trd

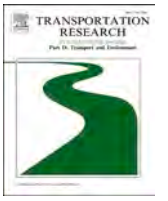

Spatio-temporal vulnerability of high-speed rail line network in China

Tao Li [a], Yu Qin [b], Mengqiao Xu [b], Yanjie Zhou [a,*], Lili Rong [b]

[a] School of Management, Zhengzhou University, Zhengzhou 450001, China
[b] School of Economics and Management, Dalian University of Technology, Dalian 116024, China

ARTICLE INFO

Keywords:
High-speed rail line
Spatio-temporal characteristic
Critical line
Vulnerability regionalization
Gravity model

ABSTRACT

Previous literature mainly focuses on the vulnerability of high-speed rail network (HSRN) at station level. High-speed rail (HSR) lines fail frequently due to disasters, which can cause a cascading effect between lines. We propose a novel method to assess the vulnerability of HSR line network (HSRLN) from the spatio-temporal perspective. To do that, the lines are described by stations, and the relations between lines are defined by train scheduling data. Then, we use the passenger volume and travel time cost between lines to assess HSRLN's vulnerability with disasters' spatio-temporal characteristics. Finally, the HSRLN in China is taken as a case. When a disaster occurs at 11:00 and lasts 6 h or 9 h, it can cause a large vulnerability. The critical lines always cover the Beijing-Shanghai and Shanghai-Kunming lines, while the regions with high-level vulnerability are mainly distributed in the Yangtze River Delta.

1. Introduction

High-speed rail, like civil aviation, has become a convenient and fast mode of transportation chosen by many people (Albalate & Bel, 2012; Sun et al., 2021; Wandelt et al., 2023b; Zhang et al., 2018a). Currently, more than 40 countries are operating or planning to build HSR (Li et al., 2021; URL, 2023). HSR has been operated as a network after decades of rapid development, consisting of many HSR lines since the opening and operation of the first HSR line, the Tokyo-Osaka line in 1964 (Jiao et al., 2017). Furthermore, the development of HSRN in many countries was not halted by the pandemic. For example, the length of HSRN in China grew from 35,000 km in 2019 to 42,000 km in 2022. Globally, the length of HSRN has increased from 44,000 km in 2017 to about 59,000 km in 2022, an increase of nearly 34.1 % during this period according to the statistics by UIC in 2023. As we all know, HSR also has a significant impact on human travel habits with the increase in network length (Yang & Zhang, 2012). For example, more than 2 billion travelers in 2019 chose HSR as a travel tool before the pandemic. However, disasters' negative consequences for HSRN exert a significant impact on people's life and travel (Bugalia et al., 2021; Read et al., 2019; Wang et al., 2022).

With the scale expansion of HSRN, more HSR lines may experience disasters and consequently suffer serious consequences (Chen & Wang, 2019; Jiao et al., 2020; Sanchis et al., 2020; Wandelt et al., 2021). In other words, HSRN may be composed of a few simple HSR lines at the early development stage, covering only a small area. After decades of development, many intertwined HSR lines make up the present HSRN, covering a wide area (Wang, 2019). This will increase the chances of HSRN being exposed to disasters. Furthermore, the consequences of a disaster can spread along some HSR lines to other related lines (Deng et al., 2018). For example, the heavy

* Corresponding author.
E-mail address: ieyjzhou@zzu.edu.cn (Y. Zhou).

https://doi.org/10.1016/j.trd.2024.104338
Received 27 March 2024; Received in revised form 15 July 2024; Accepted 15 July 2024
Available online 20 July 2024

Nomenclature

HS	High-speed
HSR	High-speed rail
HSRN	High-speed rail network
HSRLN	High-speed rail line network
GDP	Gross domestic product
l_i	High-speed rail line i
s_i	High-speed rail station i
G	High-speed rail line network G
L	Set of high-speed rail lines
E	Set of edges between lines
F	Set of edge weights with train frequency
T	Set of edge weights with travel time
P	Performance of high-speed rail line network
pf_{ij}	Passenger volume from line l_i to l_j
at_{ij}	Travel time cost from line l_i to l_j
or_{ij}	Occupancy rate of the trains from l_i to l_j
Pop_i	Population of the regions covered by l_i
GDP_i	GDP of the regions covered by l_i
D_{ij}	Distance between stations covered by l_i and l_j
n_{l_i}	Number of stations covered by l_i
θ_{ij}	Accessibility status between l_i and l_j
at	Total running time of the trains from line l_i to l_j
at	Total transfer time from line l_i to l_j
m	Transfer times from l_i to l_j
tt	Time of each transfer from l_i to l_j
haz_i	A disaster i
$t^h_{haz_i}$	Occurrence time of the disaster i
$t^d_{haz_i}$	Influence duration of the disaster i
c_{haz_i}	Occurrence location of the disaster i
r_{haz_i}	Influence scope of the disaster i
ts_{tr_i}	Failure status of the train tr_i
ss_{si}	Failure status of the station s_i
ls_{l_i}	Failure status of the line l_i
P_{no}	Performance of under its normal operation
P_{haz_j}	Performance of HSRLN under the disaster haz_j
V_{haz_j}	Vulnerability of HSRLN under the disaster haz_j
pl_{l_i}	Performance loss caused by the failure of the line l_i
reg_x	Unit of vulnerability regionalization
SDV	Variance of the vulnerability corresponding to all units
SDC	Sum of the variances of all classifications
GVF	Goodness of variance fit

rainstorm in Zhengzhou on July 20, 2021, led to the failure of the HSR stations located in Zhengzhou, and caused the failure of the Beijing-Guangzhou, Xuzhou-Lanzhou, Zhengzhou-Xiangyang, and other HSR lines. Thousands of high-speed (HS) trains passing through these lines were suspended, and tens of thousands of passengers were stranded at these HS stations.

Therefore, ensuring the security of HSRN has not only been highly valued by related administrations but has attracted the attention of related scholars (Janić, 2018; Bugalia et al., 2020; Hu et al., 2020). For example, the "14th Five-Year Development Plan of Modern Comprehensive Transportation System" issued by the State Council of China centers the safety enhancement of HSRN as an important goal and directive for development. Moreover, the number of research about HSRN security has increased by ten times in the last decade according to the statistic from 'Web of Science'. Most of the literature regards the vulnerability analysis of HSRN as the key solution for enhancing its safety (Ilalokhoin et al., 2023; Khademi et al., 2021; Li and Rong, 2022; Wandelt et al., 2021, 2023a), because HSRN's vulnerability is an inherent attribute, which can reflect its sensitivity to disasters. The impacts of disasters on HSRN and the vulnerable elements in HSRN can be effectively identified from the vulnerability perspective. Therefore, the issue on the vulnerability of HSRN has become a hot topic in the field related HSR (Rodríguez-Núñez & García-Palomares, 2014; Nicholson et al., 2016).

At present, various methods for network modeling and vulnerability assessment of HSRN have been proposed by different

researchers, playing an important role in improving the security of HSRN (Chen & Jiang, 2019; Hong et al., 2022). Firstly, HSRN is usually described as a station-based network in which the nodes represent HSR stations. For example, Ouyang et al. (2019), Hong et al. (2020), Li et al. (2019), Hu et al. (2022), Gao et al. (2023), and Zhang et al. (2023) modeled the HSRN of China as a physical network consisting of HSR stations and tracks between stations when analyzing its vulnerability based on the schedule data of HS trains. Hong et al. (2019) and Li & Rong (2020, 2021) also described HSR stations as the nodes of HSRN, while the edges of the network denoted the service links based on HS trains running between stations. Furthermore, the centrality metrics (such as the accessibility of nodes) and structure metrics (such as the shortest path length) are often selected as the indicators of HSRN's vulnerability. For example, Zhang et al. (2016) used the shortest path length to analyze and compare the vulnerability of the HSRN located in China, Japan, and America, while Ouyang et al. (2014, 2015) assessed the HSRN's vulnerability of China by using the daily accessibility.

It is easy to find that these metrics used in previous literature can only reveal the topological vulnerability (such as the sensitivity of topology structure) of HSRN against disasters (Feng et al., 2021; Mattsson & Jenelius, 2015; Reggiani et al., 2015; Wandelt et al., 2023a). However, the vulnerability of HSRN is affected not only by the changes in its topology structure but also by the changes in its function (Li & Rong, 2021). For the planners and administrators of HSR, the topology structure of HSRN is designed to fulfill its function, which includes services for passengers. As a result, an increasing number of studies have begun to focus on the functional vulnerability of HSRN or other transportation networks. Furthermore, most previous works only analyze the static vulnerability of HSRN by taking the disasters it suffering from as a static scenario (Li & Rong, 2020). In other words, these studies ignore HSRN's component failure caused by disasters with complex spatio-temporal characteristics. The occurring time and location, and lasting time and scope of the HSRN's component failure depend on the occurring time and location, and influencing time and scope of the disaster (Xu et al., 2024), and therefore HSRN may expose different vulnerabilities when suffering from disasters at different times cross various locations (Khademi et al., 2018). For example, disasters occurring at different times cross various locations can lead to the failure of HSR trains operating at that time and location. For the HSRN in China, disasters occurring during the daytime can usually cause more train failures than those occurring at night, because there are very few trains running at night overall.

Additionally, a clear limitation of these research findings is that only the scenario of an HSR station failing independently due to disasters is taken into account (Wang et al., 2015). In fact, the failure of an HSR station often results in the failure of an HSR line or multiple HSR lines covering the station, which may further lead to the failure of other HSR lines. This is because the operation of HSRN depends on many HS trains running along an HSR line or multiple lines and crossing between different HSR stations. Therefore, when the HSR stations covered by an HSR line fail, it will not only affect the HS trains running along that line, but also affect other lines associated with that line. Then, the failures caused by a disaster can spread across different lines. From the news issued by the operation department of HSRN, it can be found that the disaster consequences are usually represented by the failure of an HSR line or multiple lines after HSRN suffering from a disaster. For example, many HSR lines are disrupted by the heavy rainstorm in Zhengzhou in 2021, and the Beijing-Shanghai HSR line, Xiamen-Shenzhen HSR line, and dozens of other lines are shut down due to Super Typhoon Lekima in 2019.

To fill these gaps with considering the security management demands, we investigate the vulnerability of HSRN from the following three issues. (1) How can the HSR lines and the relations between different lines be described when modeling the HSRN from the HSR line perspective? (2) How can the vulnerability of HSRN consisting of HSR lines be assessed under considering the complex spatio-temporal characteristics of disasters? (3) How can the critical HSR line be identified, and the differences of the vulnerability exposed by HSRN in different regions along HSR lines be recognized?

In this study, we propose a novel method to describe HSRN and assess its vulnerability from the HSR line perspective. The main contributions of our study are illustrated as follows. (1) HSRN is first described as a network consisting of HSR lines, in which an HSR line is modeled as a sequential array of multiple HSR stations. The relations between HSR lines are defined based on the HS trains running between them. (2) The passenger volume and travel time cost between HSR lines are selected as the vulnerability metrics of HSRN at the HSR line level. The method for assessing the vulnerability is developed by considering the topology structure and function of HSRLN. (3) The spatio-temporal variability of HSRLN's vulnerability is first revealed by considering the occurrence time and location, and influence duration and scope of disasters. Furthermore, multiple failure states of HSRLN's components are taken into account. (4) The method for identifying the critical HSR lines and regionalizing the vulnerability is proposed to support the accurate enhancement of HSRLN security.

The rest of this study is organized as follows. Section 2 introduces the methods of HSRLN description, vulnerability assessment,

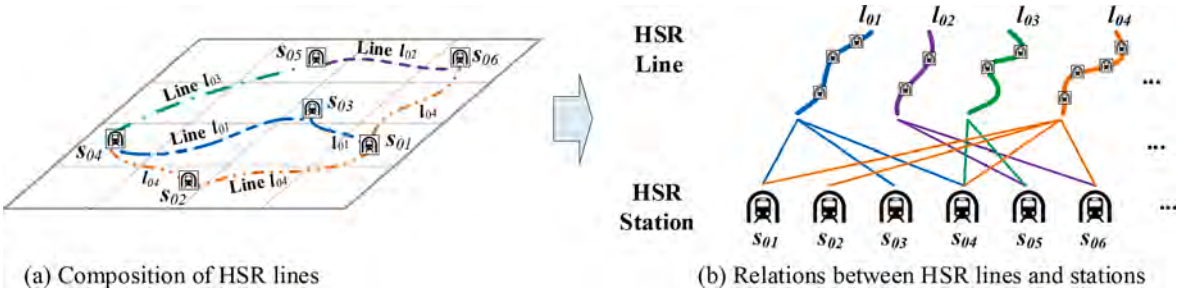

Fig. 1. An example of the description process of HSR lines.

critical line identification, and vulnerability regionalization. Section 3 shows the case of HSRLN in Mainland China from the HSR line perspective. Section 4 presents the obtained results and discussions. Section 5 illustrates the conclusions and management implications.

2. Methodology

2.1. Network description of HSRLN

Usually, a network is composed of nodes and edges according to complex network modeling method (Li & Rong, 2022; Xu et al., 2023a), and therefore the description process of HSRLN necessitates first defining the nodes and edges of the network. In this study, we define an HSR line as a node, which is composed of multiple HSR stations and tracks connecting these stations, as shown in Fig. 1(a). From the perspective of providing functions, the main purpose of constructing an HSR line is to achieve effective connections between several HSR stations covered by the line, and therefore an HSR line l_x can be described as a sequential array of multiple HSR stations, such as $l_x=(s_i,s_j,\ldots,s_y)$, illustrated in Fig. 1. The relation between HSR stations and lines is many-to-many. In other words, an HSR station can be covered by multiple HSR lines and a line can cover multiple HSR stations, as shown in Fig. 1(b). For example, the line l_{01} in Fig. 1 is composed of the stations s_{04}, s_{03}, s_{01}, and the blue dotted line connecting these stations, which can be described as $l_{01}=(s_{04}, s_{03},s_{01})$, and the station s_{04} can be covered by the line l_{01}, l_{03}, l_{04}.

The edges between HSR lines are defined based on HS trains running with HSRN. If an HS train crosses two HSR lines, there is an edge between these two lines, because an HSR line is described by multiple HSR stations, whether an HSR line is crossed by an HS train can be determined by whether the train passes through the HSR stations covered by the line. If an HS train passes through two HSR stations covered by an HSR line, then we assume that the train crosses the line. Afterwards, the relation between HSR lines and HS trains can be obtained based on the relation between HSR stations and lines and the relation between HSR stations and HS trains, illustrated in Fig. 2. For example, the HS train *D001* in Fig. 2 passes through the HSR station s_{03} and s_{01}, s_{04} and s_{05}, and these stations are respectively covered by the HSR line l_{01} and l_{03} so these two lines are crossed by *D001*. Then there is an edge between the lines l_{01} and l_{03}. However, if the lines l_{01} and l_{02} cannot be passed through by the same train, there is no edge between them.

Furthermore, the HSRLN can be described as $G=(L, E, F, T)$ in which $L=\{l_x \mid 0 < x \le n\}$ represents the set of HSR lines, n is the number of HSR lines, $E=\{e_{xy} \mid 0 < x,y \le n, x \ne y\}$ denotes the set of edges between HSR lines, $F=\{f_{xy} \mid 0 < x,y \le n, x \ne y\}$ represents the set of edge weights with HS train frequency, and $T=\{t_{xy} \mid 0 < x,y \le n, x \ne y\}$ denotes the set of edge weights with travel time by HS trains, indicated by the in-vehicle time. For example, the set of HSR lines, L, can consist of the line l_{01}, l_{02}, l_{03}, l_{04}, and the set of edges, E, can consist of the edge e_{13} *connecting* l_{01} to l_{03}, e_{14} *connecting* l_{01} to l_{04}, and so on, illustrated in Fig. 1 and Fig. 2. The HS train frequency weight of an edge connecting a pair of HSR lines indicates the number of trains crossing these two lines, and the travel time weight of the edge indicates the shortest running time between these two lines by HS trains. In other words, the travel time indicates the shortest time a train takes to depart from a station of one line to reach a station of another line. For example in Fig. 2, f_{13} represents the train frequency weight of the edge e_{13} connecting the line l_{01} to l_{03}, equal to 1, and t_{13} represents the travel time weight of e_{13} between l_{01} and l_{03} by the train *D001*. As shown in Fig. 2, the train *D001* arrives at the station s_{01} at time *t21*, meaning that it departs from the line l_{01} at time *t21*, and departs from the station s_{04} at time *t24*, meaning that it arrives at the line l_{03} at time *t24*. Therefore, the travel time weight of the edge e_{13} between l_{01} and l_{03}, t_{13}, is equal to *t24-t21*.

2.2. Metric of vulnerability

From the supply–demand perspective, the basic function of various transportation networks is to provide customers with convenient travel services. HSRLN is built and developed for the function of providing services. In other words, the function of HSRLN can be described as a service output over connected HSR lines. The service flow between HSR lines is ultimately reflected by passenger flow, and therefore maintaining this service or passenger flow is the function of HSRLN. Furthermore, the ability to maintain this passenger

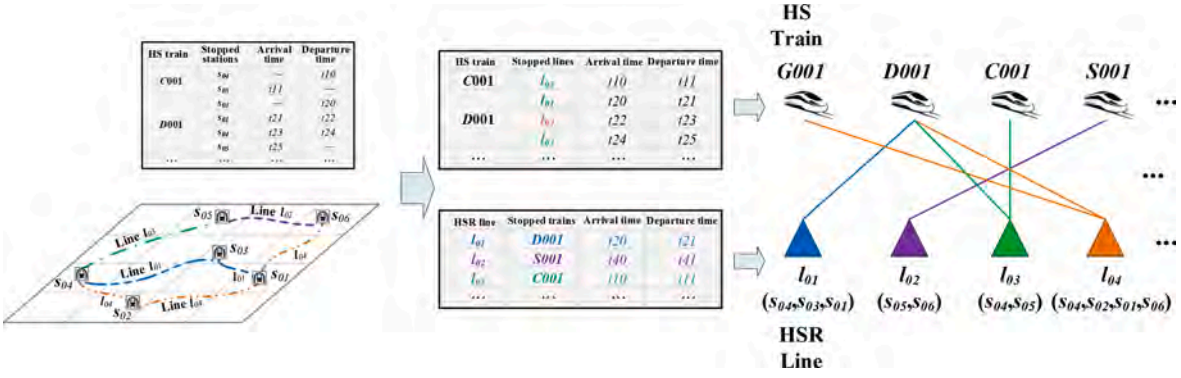

Fig. 2. A description example of the relation between HSR lines and HS trains based on train schedule data.

flow is defined as the performance of HSRLN from the perspective of its function feature (Mattsson & Jenelius, 2015; Li & Rong, 2021). When suffering from disasters, the HSRLN's performance will be affected, exposing its vulnerability.

In this study, the vulnerability of HSRLN can be defined as the loss degree of HSRLN's performance due to disasters based on the vulnerability definition of transportation in previous literature (Mattsson & Jenelius, 2015; Hong et al., 2020; Li & Rong, 2021, 2022; Zhang et al., 2023). In other words, the large performance loss of HSRLN caused by disasters indicates that it is more sensitive to disasters and exposes a large vulnerability. Thus, the vulnerability of HSRLN is determined by its performance loss. To assess the vulnerability of HSRLN, we first need to measure its performance and then calculate its performance loss caused by disasters. Therefore, the performance can be selected as the metric of the vulnerability. The passenger volume and travel time cost can be used to reflect the performance of HSRLN since its ability to maintain passenger flow depends on the volume and the cost (Sun et al., 2017; Jiao et al., 2020; Wandelt et al., 2023a; Li et al., 2024). Based on previous literature (Jiao et al., 2020; Li & Rong, 2020, 2021, 2022), the performance of HSRLN, P can be denoted as,

$$P = \frac{1}{n(n-1)} \sum_{i=1,i\neq j}^{n} \sum_{j=1,j\neq i}^{n} \frac{pf_{ij}}{at_{ij}} \tag{1}$$

where pf_{ij} represents the passenger volume from HSR line l_i to l_j, and at_{ij} represents the travel time cost from l_i to l_j. pf_{ij} and at_{ij} can be calculated by the following steps and equations, in which pf_{ij} indicates the train frequency with relative occupancy rate and at_{ij} indicates the travel time in hours. Then the performance of HSRLN, P, indicates the passenger volume per unit of travel time cost, that is, the number of trains per hour.

In the normal case, the more frequent the train operation between two HSR lines and the higher the train occupancy rate, the greater the passenger volume between these two lines. Therefore, the passenger volume between two HSR lines is related to the frequency and occupancy of the trains running between these two lines. The train frequency can be obtained from the set of edge weights of HSRLN, and the train occupancy is typically related to the travel demand that can often be estimated by the gravity model as a whole in the case of limited data (Zhang & Zhang, 2016; Zhang et al., 2018b; Yu et al., 2021; Li & Rong, 2021). In gravity model, the closer the distance between two HSR lines and the larger the population and the GDP (Gross Domestic Product) of the regions covered by these lines, the higher the demand for travel between the two lines and the greater the occupancy rate of the trains running between these lines. On the basis of the above analysis, the passenger volume, pf_{ij}, can be calculated as,

$$pf_{ij} = tf_{ij} \times \overline{or}_{ij} \times \theta_{ij} \tag{2}$$

$$\overline{or}_{ij} = \frac{\log(or_{ij})}{\log(\max(or))} \tag{3}$$

$$or_{ij} = \gamma \frac{\left((Pop_i)^{\alpha} \times (GDP_i)^{\beta}\right) \times \left(\left(Pop_j\right)^{\alpha} \times \left(GDP_j\right)^{\beta}\right)}{\left(D_{ij}\right)^{\lambda}} \tag{4}$$

$$D_{ij} = \frac{1}{n_{l_i} n_{l_j}} \sum_{s_x \in l_i} \sum_{s_y \in l_j} D_{s_x s_y} \tag{5}$$

$$Pop_i = \frac{1}{n_{l_i}} \sum_{s_x \in l_i} Pop_{s_x} \tag{6}$$

$$GDP_i = \frac{1}{n_{l_i}} \sum_{s_x \in l_i} GDP_{s_x} \tag{7}$$

$$\theta_{ij} = \begin{cases} 1 & \textit{The line i is accessible to line j} \\ 0 & \textit{The line i is inaccessible to line j} \end{cases} \tag{8}$$

where tf_{ij} represents the train frequency from HSR line l_i to l_j, $\overline{or}_{ij}$ represents the relative value of the occupancy rate or_{ij} of the trains running from l_i to l_j, max(or) is the maximum value of the occupancy rate of the trains running between all pairs of the lines, Pop_i and Pop_j respectively indicate the population of the regions covered by l_i and l_j, GDP_i and GDP_j respectively indicate the GDP of the regions covered by l_i and l_j, D_{ij} represents the spatial distance between l_i and l_j, $D_{s_x s_y}$ represents the spatial distance between the HSR station s_x covered by l_i and the HSR station s_y covered by l_j, n_{l_i},n_{l_j} respectively indicate the number of HSR stations covered by l_i and l_j, Pop_{s_x},GDP_{s_x} respectively indicate the population and GDP of the station s_x covered by l_i, γ, α, β, and λ respectively indicate the gravity constant, the control parameter of the population, GDP, and spatial distance, and θ_{ij} represents the accessibility status between l_i and l_j. If the HSR line l_i is directly accessible to l_j without transferring, tf_{ij} is equal to the train frequency weight of the edge connecting them, f_{ij}. Since an HSR line is described by a sequential array of multiple HSR stations, a line can consist of multiple stations and there is a clear difference in the number of stations covered by different lines. To avoid the influence of that difference on the obtained results, we adopt the mean value for calculating GDP_i, GDP_j and D_{ij}. In other words, GDP_i is calculated by the average GDP of the regions covered by l_i, and D_{ij}

is calculated by the average spatial distance between the HSR stations covered by l_i and the stations covered by l_j.

Based on previous literature, the travel time cost can be described as the shortest travel time, composed of the pure running time of trains (in-vehicle time) and transfer time at the transfer stations, and measured in hours (Corman et al., 2014; Gentile and Noekel, 2016; Wang et al., 2016; Sun et al., 2017; Jiao et al., 2020; Wandelt et al., 2023a; Li et al., 2024). The pure running time refers to the time passengers spend on trains and transfer time refers to the time passengers spend on transferring from one train to another at transfer stations. Thus, the travel time cost, at_{ij}, can be denoted as,

$$at_{ij} = \min\left(at_{ij}^{r} + at_{ij}^{t}\right) \tag{9}$$

$$at_{ij}^{r} = t_{iz_1} + t_{z_1 z_2} + \cdots + t_{z_m j} \tag{10}$$

$$at_{ij}^{t} = m \times tt \tag{11}$$

where at, at respectively indicate the total running time of the trains and the total transfer time from the HSR line l_i to l_j at the transfer station s_z, m, tt respectively indicate the transfer times and the time of each transfer from l_i to l_j. If the HSR line l_i is directly accessible to l_j without transferring, at and m are equal to 0, and at is equal to the travel time weight of the edge connecting them, t_{ij}. If the HSR line l_i is inaccessible to l_j, at_{ij} is infinite.

2.3. Assessment of vulnerability

According to the vulnerability definition of HSRLN, the prerequisite for assessing the vulnerability is to first identify the performance loss of HSRLN in a disaster scenario. Once a disaster occurs, the HSR trains and stations within HSRLN will be negatively affected, and the HSR lines will fail. Then the edges between these lines and the weights of these edges within HSRLN will change and the passenger volume and travel time cost within the network will also change. Therefore, the performance loss of HSRLN is related to the disaster it suffers and the failure status of the trains, stations, and lines within the network. Firstly, the disasters suffered by HSRLN have a typical complexity with spatio-temporal characteristics. The impact of a disaster on HSRLN's performance varies across different occurrence time and location, influence duration and scope of the disaster. For example, a disaster occurring in southeast China with dense HSR lines and lasting for a long time often has a greater impact on HSRLN than one occurring in western China with sparse HSR lines and lasting for a short time. In this study, a disaster, haz_i, is described as,

$$haz_i = \left(t_{haz_i}^{h}, t_{haz_i}^{d}, c_{haz_i}, r_{haz_i}\right) \tag{12}$$

where $t_{haz_i}^{h}$,$t_{haz_i}^{d}$,c_{haz_i},r_{haz_i} represent the occurrence time, influence duration, occurrence location, and influence scope of haz_i, respectively.

Secondly, the failure status of the trains, stations, and lines within HSRLN can be divided into different categories according to the disaster scenarios. For example, the failure status of trains can be categorized into limit-speed operation and suspension, described as ts_{tr_i},

$$ts_{tr_i} = \left(haz_j, sp_{tr_i}\right) \tag{13}$$

where sp_{tr_i} represents the percentage of the speed limit of the train tr_i under the disaster haz_j. If sp_{tr_i} is equal to 1, the failure status of tr_i is suspension. Similarly, the failure status of stations can be categorized into functional failure and physical failure, described as ss_{si},

$$ss_{s_i} = \left(haz_j, pf_{s_i}\right) \tag{14}$$

$$pf_{s_i} = \begin{cases} 1 & Functionalfailure \\ 2 & Physicalfailure \end{cases} \tag{15}$$

where pf_{si} represents the failure status of the station s_i under the disaster haz_j. If pf_{si} is equal to 2, the failure status of s_i is complete suspension. However, the failure status of an HSR line depends on the failure status of the trains running on the line and the stations covered by the line. If all the stations covered by a line or all trains running on a line are completely out of service, the line is also completely out of service. The failure status of lines can be categorized into partial and complete outage, described as ls_{l_i},

$$ls_{l_i} = \left(haz_j, lf_{l_i}\right) \tag{16}$$

$$lf_{l_i} = \begin{cases} 1 & Completeoutage \\ \sigma \in (0,1) & Partialoutage \end{cases} \tag{17}$$

where lf_{l_i} represents the failure percentage of the line l_i under the disaster haz_j. If lf_{l_i} is equal to 1, the failure status of l_i is complete outage.

Finally, the nodes, edges and the weights of these edges within HSRLN under the disaster haz_j can be remodeled. Then the performance of HSRLN under disaster haz_j, P_{haz_j}, can be calculated by Eq.(1) and the performance loss can also be calculated. Based on the performance loss, the vulnerability of HSRLN under the disaster haz_j, V_{haz_j}, can be assessed,

$$V_{haz_j} = \frac{P_{no} - P_{haz_j}}{P_{no}} \tag{18}$$

where P_{no} represents HSRLN's performance under its normal operation before suffering from the disaster haz_j.

2.4. Critical lines identification and vulnerability regionalization

The important purpose of assessing the vulnerability of HSRLN is to reduce the impact of disasters on it by protecting the critical lines and areas within the network. The critical HSR lines are the lines whose failure causes a larger performance loss to HSRLN than the failure of other lines. In this study, the critical lines can be identified by the enumeration method which assumes that each line of HSRLN fails in turn, and then the performance loss caused by the failure, pl_{l_i}, can be calculated as,

$$pl_{l_i} = P_{no} - P_{l_i} \tag{19}$$

where P_{l_i} represents HSRLN's performance under the complete outage of the line l_j. The critical lines can be identified by comparing the performance loss pl_{l_i} corresponding to each line.

The identification of critical lines is only to recognize the role of these lines in HSRLN, while the vulnerability regionalization is to recognize the role of the regions along HSR lines in the network. In other words, the difference between the regions with high vulnerability and the regions with low vulnerability can be distinguished by dividing the vulnerability level of all regions along HSR lines. The process of vulnerability regionalization includes the following steps.

Step 1: Set the unit of the regionalization, reg_x. The regionalization unit is the smallest area that can be shown on a regionalization map. The prefecture-level city where the stations covered by HSR lines are located is selected as the regionalization unit in this study.

Step 2: Select the indicator of the regionalization. The vulnerability that HSRLN exposes on the regionalization units is selected as the regionalization indicator since the purpose of this study focuses on the vulnerability regionalization. Specially, the vulnerability, V_{reg_x}, exposed by HSRLN under the complete failure of all lines and trains passing through a regionalization unit after a disaster, is used as the basis for regionalizing,

$$V_{reg_x} = \frac{P_{no} - P_{reg_x}}{P_{no}} \tag{20}$$

where P_{reg_x} represents HSRLN's performance under the disaster occurring in the unit reg_x and causing the complete failure of all lines and trains passing through reg_x.

Step 3: Visualize the regionalization results. The natural breakpoint method is applied to determine the classification of regionalization units based on the magnitude and variance of the vulnerability corresponding to all units and the sum of the variances of different classifications (Chen et al., 2023). The variance of the vulnerability corresponding to all units, *SDV*, and the sum of the variances of all classifications, *SDC*, can be calculated as,

$$SDV = \frac{1}{n_{reg}} \sum_{x=1}^{n_{reg}} \left(V_{reg_x} - \overline{V_{reg}}\right)^2 \tag{21}$$

$$SDC = \sum_{y=1}^{nc} \frac{1}{n_{reg}^{y}} \sum_{x=1}^{n_{reg}^{y}} \left(V_{reg_{xy}} - \overline{V_{reg_y}}\right)^2 \tag{22}$$

$$GVF = 1 - \frac{SDC}{SDV} \tag{23}$$

where n_{reg} and nc respectively indicate the number of regionalization units and their classifications, $\overline{V_{reg}}$ represents the mean of the vulnerability corresponding to all units, $n\,y\,reg$ represents the number of the units within the classification y, $V_{reg_{xy}}$ and $\overline{V_{reg_y}}$ respectively indicate the vulnerability corresponding to the unit reg_x with the classification y and the mean of the vulnerability corresponding to all units with the classification y, and *GVF* represents the goodness of variance fit. In general, a *GVF* greater than 0.7 is acceptable. Finally, the regionalization map of HSRLN's vulnerability can be obtained and visualized based on the classification and its criteria of the units.

3. Case study

3.1. Case and data

To verify the validity of the proposed method, the HSRLN located in Mainland China is taken as the case study. As of May 2021, the HSRLN of Mainland China has covered 22 provinces, 5 autonomous regions, and 4 municipalities, which includes more than 1,300

HSR stations. In this study, we select the stations located in prefecture-level and above cities and trains passing through these stations as the components of the HSRLN. There are 263 prefecture-level and above cities operating HSRLN.

Furthermore, there are five types of data used for the case study, containing the HS train timetable, HSR line, HSR station coordinate, urban socio-economic statistics, and vector map. First, the train timetable can be obtained from 12,306 China Railway. In this paper, we use the daily train timetable in May 2021. Second, the data of the HSR line comes from the planning map of the medium-long term HSRN issued by the Chinese government as of May 2021. Third, the coordinate data of HSR stations is acquired from Google Maps as of May 2021. Finally, the urban socio-economic statistics can be collected from the China city statistical yearbook in 2022.

3.2. Description of the HSRLN

We collect 109 HSR lines, among which 8 lines are isolated and not related to other lines, and 7 lines are duplicates and subsets of other lines, and therefore these 15 lines are eliminated from the 109 lines and the stations covered by the 8 isolated lines are also eliminated. Finally, the HSRLN in Mainland China consists of 94 lines that cover 251 stations and 5,144 trains running on a certain day, as shown in Fig. 3 illustrating the relations between these lines, stations, and trains.

As shown in Fig. 3, the HSR lines located in central and eastern regions are usually busier and have a higher frequency of trains passing them than others. There are only a few lines on which the frequency of trains exceeds 500, and most of these lines are hub lines and longer lines that cover a larger number of stations. For example, the Beijing-Guangzhou line (blue line located in the middle of Fig. 3) covers 24 stations and the Shanghai-Kunming line (blue line lying flat in the lower middle of Fig. 3) covers 23 stations. However, most of the lines' length is relatively short, covering fewer stations, and the frequency of trains passing them is usually less than 500.

Furthermore, the left part of Fig. 4 reveals that the number of stations covered by most of the lines is no more than 4 and the number of lines covering more than 7 stations is small as a whole. The right part of Fig. 4 shows that there is a certain linear relation between the number of stations covered by a line and the train frequency on it, which means that the more stations covered by a line, the higher the frequency of trains running on it. But the lines covering a relatively small number of stations may also be stopped by many trains. For example, the Beijing-Shanghai line (red line in Fig. 3) covers only 18 stations while the frequency of trains running on it is the highest. Fig. 5 illustrates that more than half of the 5,144 trains only pass through 2 lines, running less than 5 h, while a small number of trains only pass through more than 6 lines, running more than 16 h.

There are 682 edges between these 94 lines in the HSRLN, as shown in Fig. 6. As can be seen from Fig. 6, the cross-provincial lines, which connect economically developed and densely populated regions, often have greater node degree. For example, the Beijing-Guangzhou, Beijing-Shanghai, and Shanghai-Kunming lines play the role of bridge throughout the north and south, the east and west in the HSRLN, making up important parts of the "four vertical and four horizontal" and "eight vertical and eight horizontal" channels in the network. However, the lines connecting the stations located in the same provincial region usually have few connecting edges, such as the Wuhan-Huanggang, Dandong-Dalian, and the branches of other lines.

The probability distribution of the degree of the lines as a node in the HSRLN tends to follow the characteristic of power law

Fig. 3. Spatial distribution of the HSR lines in the frequency of trains passing them.

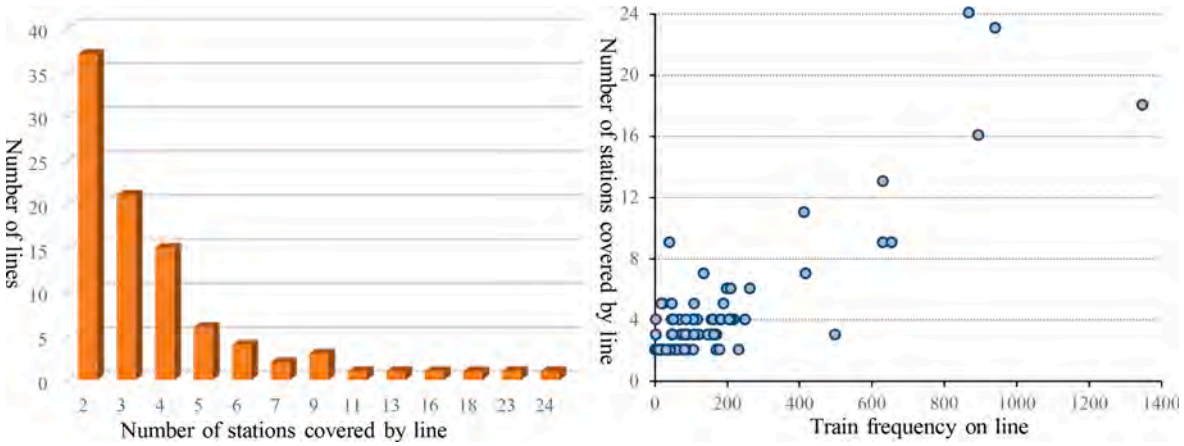

Fig. 4. Distribution of the HSR lines frequency in the number of stations they include, and the relations between the number and the frequency of trains passing a line.

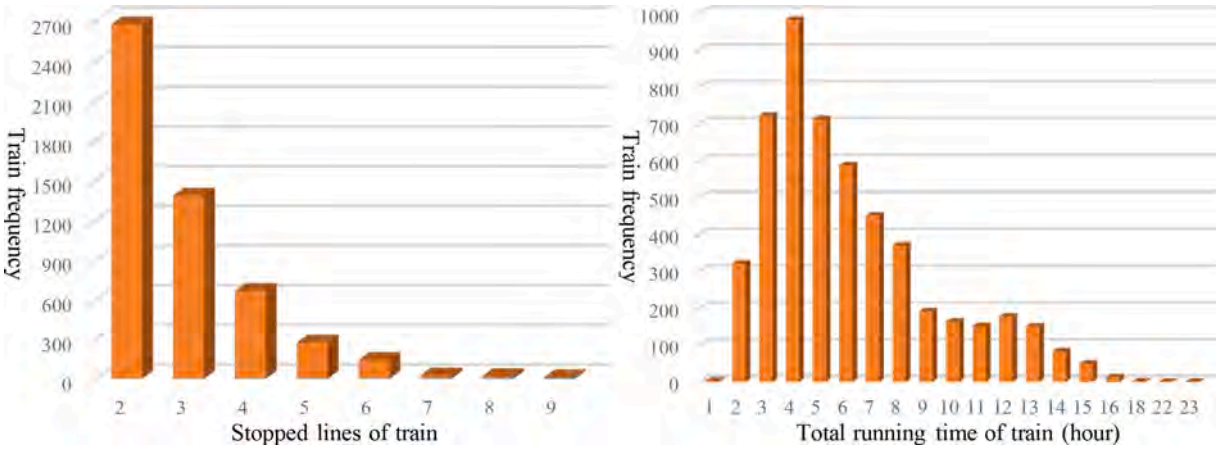

Fig. 5. Distribution of the HSR lines frequency in the number of stations they include, and the relations between the number and the frequency of trains passing a line.

distribution, illustrated in the left part of Fig. 7. In other words, the degree of most lines is relatively small while only a few lines have a great degree. Additionally, there is a clear positive correlation between the degree of the line and the train frequency on it, meaning that the lines with a great degree can be stopped by many trains in the HSRLN, as shown in the right part of Fig. 7. Table 1 reveals that each line in the HSRLN covers at least 4 stations and is directly connected with at least 14 other lines on average. Although the lines are busy as a whole, their busyness varies greatly. That is to say that the maximum and minimum of train frequency on the lines are 1,350 and 2, respectively.

4. Results

Referring to previous literature on the evaluation of train occupancy rate and passenger flow demand based on the gravity model, the gravity constant, the control parameter of the population, GDP, and spatial distance are set as 1 for balancing their impacts on the calculated results (Zhang & Zhang, 2016; Zhang et al., 2018b; Yu et al., 2021; Li & Rong, 2021). Moreover, the transfer time at each transit station is set as 0.5 h, referencing previous research and acknowledging that many stations have set up fast transit channels (Wang et al., 2016; Li & Rong, 2020). The performance of the HSRLN in Mainland China under normal operation is 66.81, indicating that there are 66.81 HS trains with relative occupancy rate per unit hours between all lines in the network. In other words, there are an average of 66.81 trains running between all lines in the HSRLN every hour. The ability to maintain this "train flow" can reflect the performance of the HSRLN in normal operation.

4.1. Spatio-temporal vulnerability variability of the HSRLN

The disaster scenario needs to be set first when analyzing the vulnerability of the HSRLN. Firstly, the Monte Carlo method is used to

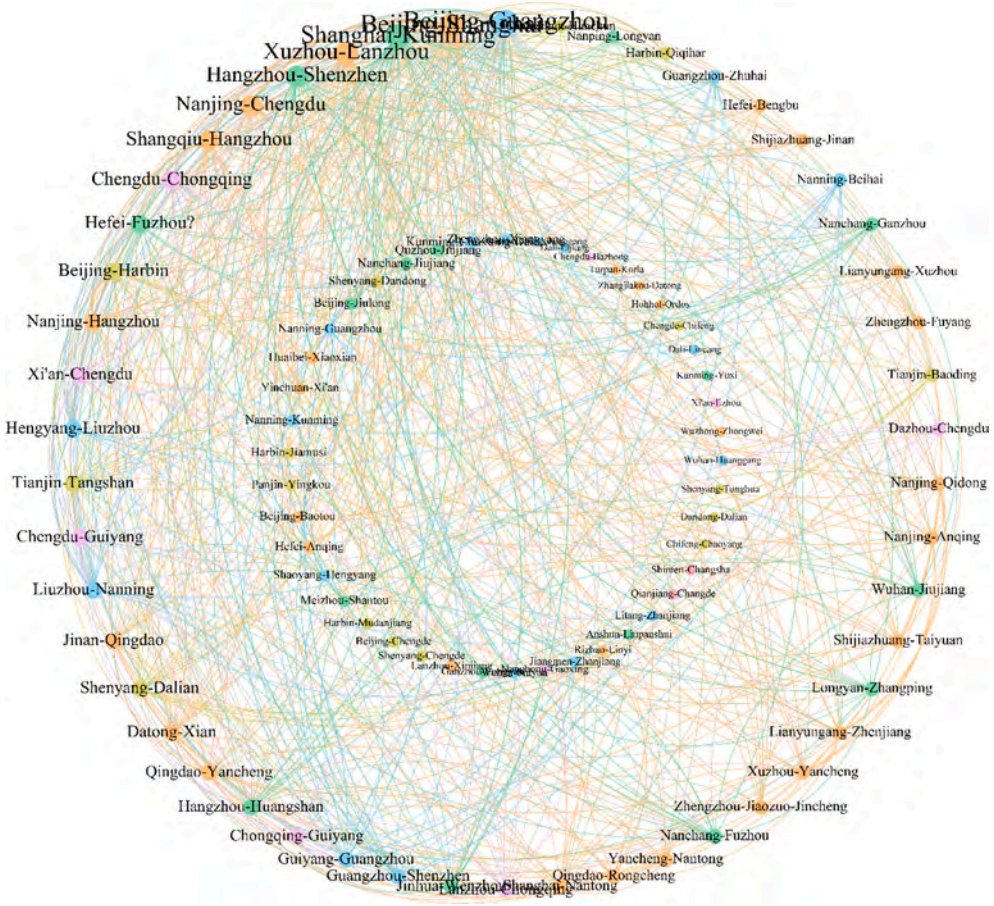

Fig. 6. Visualization of the HSRLN located in Mainland China. The larger size of the text and dots indicate the greater degree of the line as a node in the HSRLN, the curve represents the edges between lines.

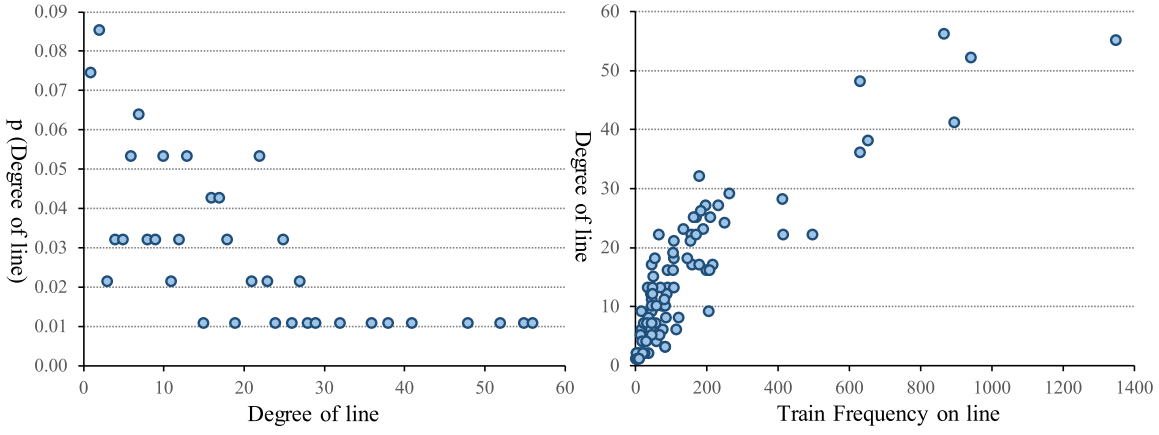

Fig. 7. Distribution of the HSR lines frequency in the number of stations they include, and the relations between the number and the frequency of trains passing a line.

simulate the disaster with random characteristics that the occurrence time $t^h_{haz_i}$ and location c_{haz_i}, influence duration $t^d_{haz_i}$ and scope r_{haz_i} are random, and 10 types of random disaster scenarios are set. The first type is that the disaster occurs at 0:00 and lasts for 24 h, and the other types are characterized by the occurrence time $t^h_{haz_i}$ belonging to 7:00, 11:00, or 15:00 and the influence duration $t^d_{haz_i}$ belonging to 3 h, 6 h, or 9 h. For each type of disaster scenario, its occurrence location c_{haz_i} is determined by the randomly selected lines, stations

Table 1
Basic attributes of the HSRLN.

Attribute	Number of stations covered by line	Degree of line	Train frequency on line	Number of lines stopped by train	Train-frequency weight	Travel-time weight
Maximum	24	56	1350	9	384	24.0
Average	2	1	2	2	1	0.02
Minimum	4.2	14.5	154.1	2.8	23.7	3.1

or trains, and its influence scope r_{haz_i} is determined by the fraction of the number of these lines, stations or trains to the total lines, stations or trains within the HSRLN. The fraction is set to range from 0 to 1 with an interval of 0.0125.

Furthermore, the selection of a line, a station or a train means that it is located in the scope of the disaster, and so will fail. If the failure status of a line is a complete outage, the trains passing through it will fail. If the failure status of a line is set as partial outage and the failure status of its covering stations is a physical failure, the trains passing through these stations will fail; otherwise, the trains will not be affected. If the failure status of a station is a physical failure, the trains passing through it will fail; otherwise, the trains will not be affected. In this study, the partial failure status of a train is set as only 50 % limit-speed operation, and the failure impacts of the lines and trains on the HSRLN's vulnerability are investigated separately for easy analysis.

Fig. 8 reveals that the HSRLN is more vulnerable to the random failure of lines (denoted by 'LINE' in Fig. 8) than the random failure of stations and trains (respectively denoted by 'STA' and 'TRA' in Fig. 8), caused by the random disasters. Since a line can cover multiple stations, its failure can often lead to the failure of multiple trains, which can have a great impact on the performance of the HSRLN. Additionally, the random failure of stations can result in a larger vulnerability than that of trains. This is because a station can be passing through by multiple trains. If a station fails, it can cause the failure of multiple trains.

It can be seen from Fig. 8 that the HSRLN exposes different vulnerabilities when the occurrence time and influence duration of the lines or trains failure caused by random disasters are different. Specially, when the influence duration $t^d_{haz_i}$ of the failure is 6 h and 9 h

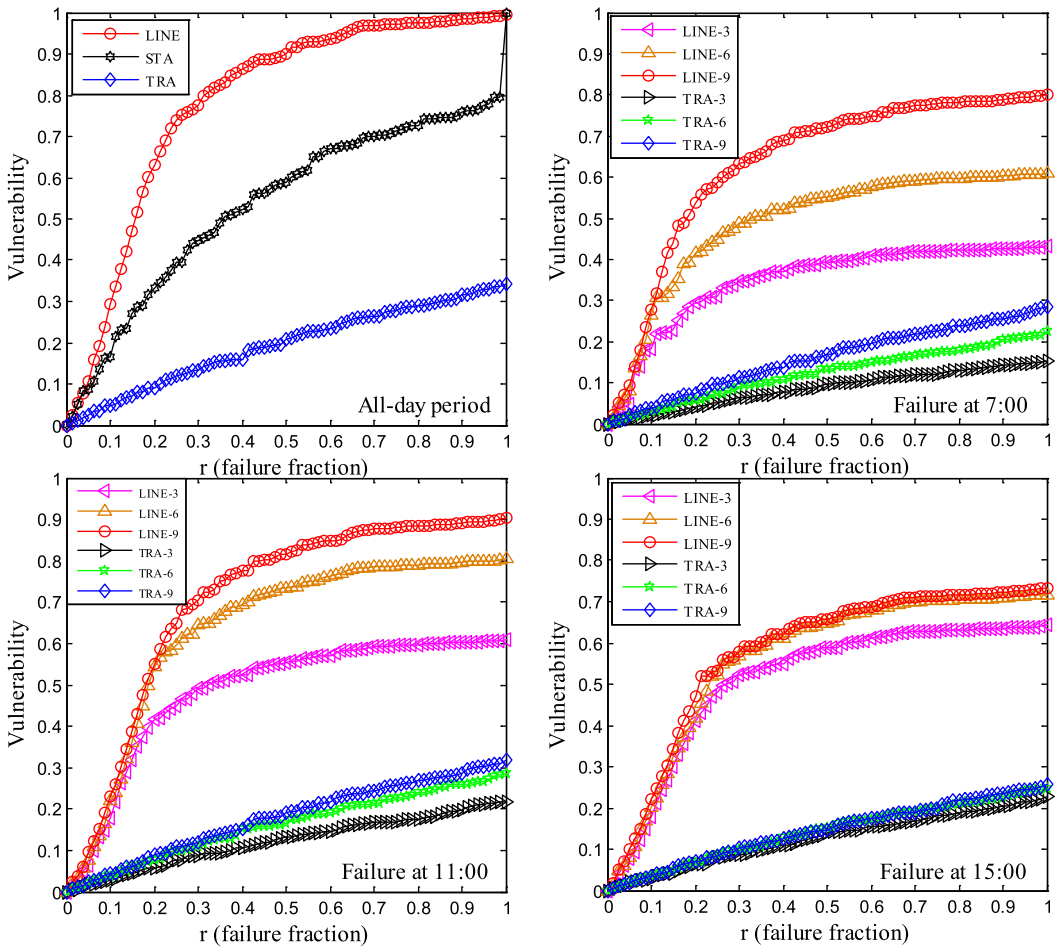

Fig. 8. Vulnerability of the HSRLN in the case of random failure of the HSR lines/stations/trains under different disaster scenarios.

(separately denoted in Fig. 8 by 'LINE-6′ and 'LINE-9′ for lines, and by 'TRA-6′ and 'TRA −9′ for trains), the random failure occurring at 11:00 of both the lines and trains can cause a greater vulnerability than that occurring at other times. When $t^d_{haz_i}$ is 3 h (denoted in Fig. 8 by 'LINE-3′ for lines, and by 'TRA-3′ for trains), the failure occurring at 15:00 can cause a large vulnerability. Furthermore, when the failure occurring at 7:00, the vulnerability exposed by the HSRLN varies greatly as $t^d_{haz_i}$ increasing, which indicates that the HSRLN's vulnerability is sensitive to the influence duration of the failure. Nevertheless, the vulnerability is slow to the increase of $t^d_{haz_i}$ when the failure occurs at 15:00.

Secondly, to simulate the disaster with malicious characteristics that the occurrence time $t^h_{haz_i}$ and location c_{haz_i}, influence duration $t^d_{haz_i}$ and scope r_{haz_i} are malicious, 10 types of malicious disaster scenarios are also set based on $t^h_{haz_i}$ and $t^d_{haz_i}$. In other words,$t^h_{haz_i}$ and $t^d_{haz_i}$ are set to be similar to the random disaster scenarios, and c_{haz_i},r_{haz_i} are respectively determined by the selected lines, stations or trains and the fraction of the number of these lines, stations or trains. However, the lines, stations or trains are selected according to their importance rather than randomly selected. When selecting a line, a station or a train in each type of malicious disaster scenario, the one with the high importance is preferred.

The importance of a line is determined by its degree (denoted by 'LINE-D' in Fig. 9) or the train frequency (denoted by 'LINE-F' in Fig. 9). The higher the degree or frequency of a line, the more important the line is. The importance of a station is determined by its degree (denoted by 'STA-D' in Fig. 9) or the train frequency (denoted by 'STA-F' in Fig. 9). The higher the degree or frequency of a station, the more important the station is. The importance of a train depends on its running time (denoted by 'TRA-R' in Fig. 9). The greater the total running time of a train, the more important it is. Moreover, the failure status of the lines and stations, and trains is set as a complete outage and suspension respectively for our examination of the serious impacts of malicious disaster scenarios.

Fig. 9 shows that the HSRLN can expose high vulnerability against a small fraction of the malicious failure, while the change in the vulnerability gradually slows down as the failure fraction increases. For example, the vulnerability of the HSRLN is close to 1 when the failure fraction is equal to 0.3, which means the network essentially loses all its performance. The failure fraction of lines is equal to about 0.05, causing the vulnerability to be about 0.8, while the failure fraction of stations is equal to about 0.6, causing the

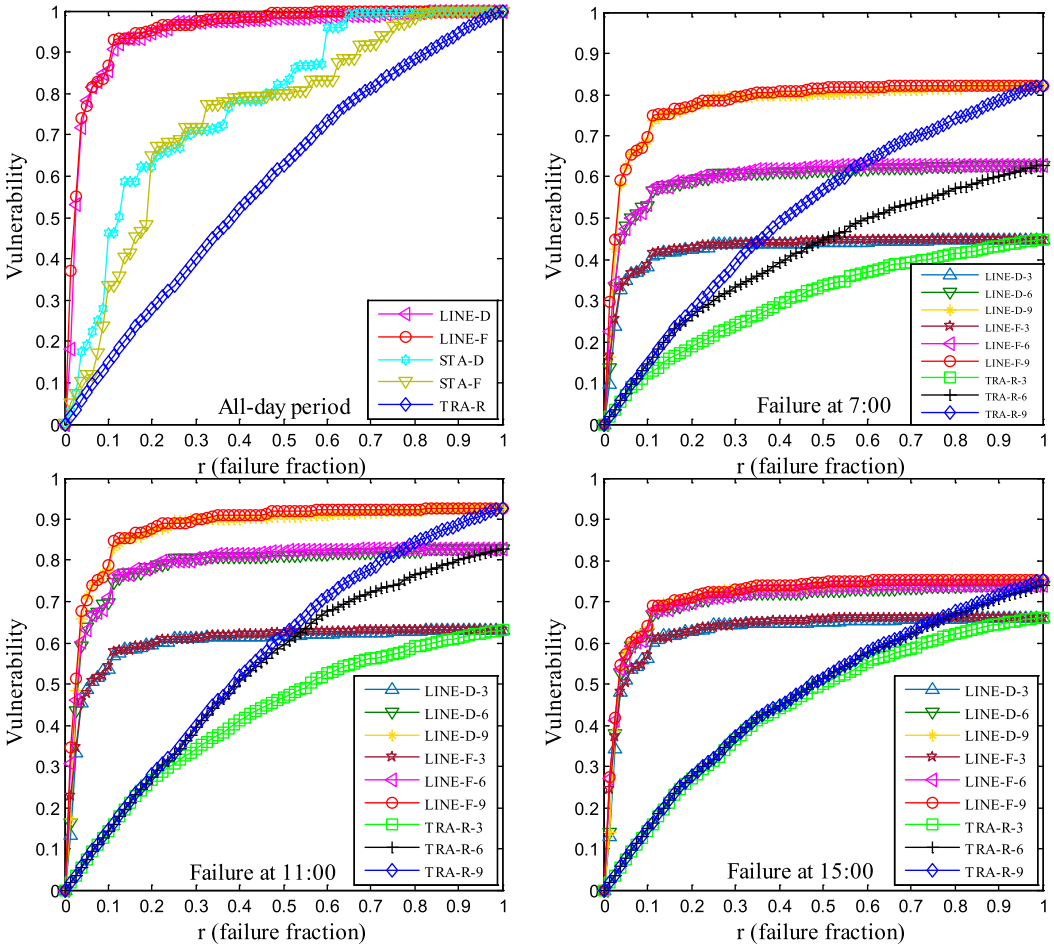

Fig. 9. Vulnerability of the HSRLN in the case of malicious failure of the HSR lines/stations /trains under different disaster scenarios.

vulnerability to be about 0.8. This reveals that the HSRLN is more vulnerable against the malicious failure of lines than that of stations. Furthermore, the HSRLN exposes larger vulnerability against the malicious failure occurring at 11:00 than that at other times when the influence duration $t^d_{haz_i}$ of the failure is 6 h and 9 h (in Fig. 9, 'LINE-D-6′ and 'LINE-F-6′ respectively denote $t^d_{haz_i}$ equal to 6 h based on the importance in the degree and train frequency for lines, 'TRA-R-9′ denotes $t^d_{haz_i}$ equal to 9 h based on the importance in the running time for trains). It is clear that the impacts of the malicious failure based on the degree and train frequency of the lines on the vulnerability is basically the same regardless of the failure occurring time, because there is an evident correlation between the line degree and train frequency on it, as shown in Fig. 7. Additionally, the vulnerability changes greatly as $t^d_{haz_i}$ increases from 3 h to 6 h when the malicious failure of lines or trains occurs at 11:00.

Thirdly, most disasters occur within a local space, which needs to be simulated based on typical disaster cases. For example, typhoons as the typical and main disaster threatening the HSRLN have always been highly emphasized by administrations. Typhoon 'Lichima' landing in China on August 10, 2019, caused the failure of dozens of lines and thousands of trains within the HSRLN. In this study, the localized disaster scenarios are set based on the typhoon 'Lichima'. That is to say, Hangzhou, Yancheng, and Qingdao are taken as the center points c_{haz_j} in the typhoon path, and the influence scope r_{haz_i} is set as 100 km and 200 km, as shown in Fig. 10. For each c_{haz_j} and r_{haz_i}, the influence time range is set as$t^h_{haz_i}$ = 0:00 and$t^d_{haz_i}$ = 24 h (0:00 ~ 24:00), $t^h_{haz_i}$=6:00 and$t^d_{haz_i}$ = 6 h (6:00 ~ 12:00), $t^h_{haz_i}$=12:00 and$t^d_{haz_i}$ = 6 h (12:00 ~ 18:00), $t^h_{haz_i}$=18:00 and$t^d_{haz_i}$ = 6 h (18:00 ~ 24:00).

Table 2 illustrates that the HSRLN can be affected differently with the changing of c_{haz_j} and r_{haz_i} when the influence time range of the typhoon is set from 0:00 to 24:00. There are 5 lines and 786 trains failure caused by the typhoon located in Hangzhou withr_{haz_i} = 100 km, resulting in the vulnerability to be equal to 0.2388. However, when its center shifts to Qingdao withr_{haz_i} = 200 km, the typhoon can cause the failure of 4 lines and 356 trains and the vulnerability to be equal to 0.1012. Hangzhou among the three centers has the greatest impact on the HSRLN's vulnerability, because the lines passing through Hangzhou play a greater role in the HSRLN, such as

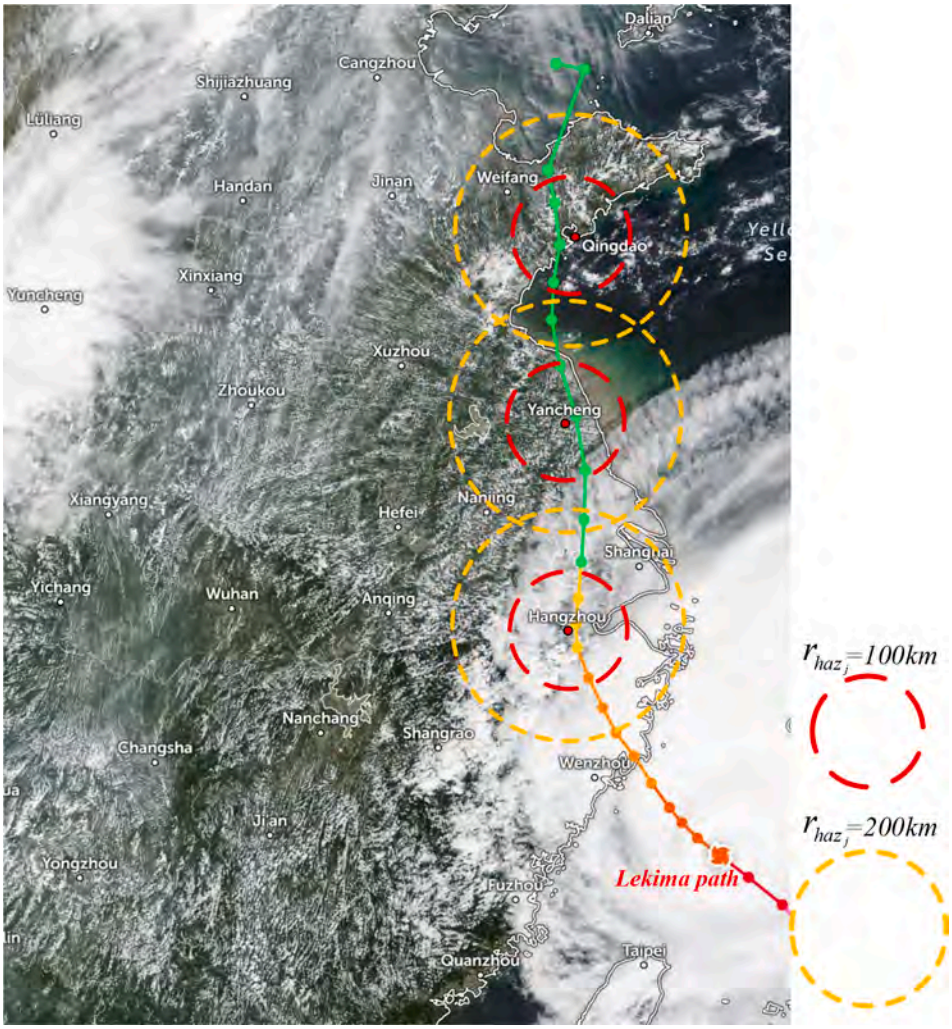

Fig. 10. Influence spaces and scopes of the disaster scenarios based on super typhoon Lekima.

the Shanghai-Kunming, Beijing-Shanghai, and Hangzhou-Shenzhen lines, compared to the lines around Yancheng and Qingdao.

Furthermore, when the spatio-temporal influence of the typhoon is different, its impact on the HSRLN's vulnerability is also different, as shown in Table 3. In other words, the influence time ranging from 12:00 to 18:00 of the typhoon located in Hangzhou can lead to a larger vulnerability (equal to 0.3297) than the other two influence time ranges, and its influence time ranging from 6:00 to 12:00 has the smallest impact on the vulnerability, regardless whether the $r_{haz_i} = 200$ km or 100 km. Nevertheless, when the typhoon's center is located in Qingdao, the impact of its influence time ranging from 18:00 to 24:00 on the vulnerability is smallest. In addition, it is not difficult to find whether the center of the typhoon is located in Hangzhou or Yancheng, or Qingdao and its influence scope is 100 km or 200 km, its influence time ranging from 12:00 to 18:00 always results in a large vulnerability. This is because there are many trains running between the lines passing through Hangzhou, Yancheng, and Qingdao during the above period. The typhoon occurring at this time can cause many trains to fail and large performance losses.

4.2. Lists of critical lines under different periods

Four different periods of the line failure are set to identify the impact of the failure influence time range on the rank list of the critical lines within the HSRLN. The periods of the line failure include the all-day period (0:00 to 24:00) and three different periods of the day (6:00 to 12:00, 12:00 to 18:00, and 18:00 to 24:00),

Table 4 reveals that a line failure under different periods and different lines failure under the same period can cause the HSRLN to expose different vulnerabilities. For example, the Beijing-Guangzhou line failure under the all-day period can result in the vulnerability to be equal to 0.1801, while its failure under the period from 12:00 to 18:00 and from 18:00 to 24:00 can result in the vulnerability to be equal to 0.1610 and 0.1105 respectively. As the period from 6:00 to 12:00, the failure of the Beijing-Guangzhou and Beijing-Harbin lines can result in the vulnerability to be equal to 0.1275 and 0.0905 respectively. This is because the number of stations covered by different lines is different, leading to different train frequencies on the lines and different relations with other lines under different periods.

Although the rank lists of the critical lines under different periods are different, some lines are always listed in the top 10 ranks under different periods. For example, the Lianyungang-Zhenjiang line is listed as the critical line under the all-day period but not under other periods. Hangzhou-Shenzhen line ranks 4th under the all-day period while it respectively ranks 5th and 3rd under the period from 6:00 to 12:00 and from 18:00 to 24:00. The rank lists always include Beijing-Shanghai, Shanghai-Kunming, Shangqiu-Hangzhou, and Beijing-Guangzhou lines. These lines are the hubs of the HSRLN, which can exert significant impacts on the network.

Furthermore, it can be seen from Table 4 that the HSRLN exposes different vulnerabilities against the line failure under the three different periods of the day. The line failure under the period from 12:00 to 18:00 always causes a larger vulnerability than that under other periods. For example, the Beijing-Shanghai line failure under the period from 12:00 to 18:00 leads to the vulnerability to be equal to 0.3141, while the failure under the period from 6:00 to 12:00 and from 18:00 to 24:00 respectively cause the vulnerability to be equal to 0.2074 and 0.2185. This is because the trains and their frequency running on a line vary across different periods.

4.3. Vulnerability regionalization on whole space

The vulnerability, V_{reg_x}, corresponding to each regionalization unit in Mainland China can be obtained by the proposed method in Section 2.4. After calculation, the maximum and minimum of V_{reg_x} are equal to 0.3043 and 0 respectively. The V_{reg_x} is equal to 0 due to the weak failure impacts of the lines and trains covered by a regionalization unit on the HSRLN's performance, which is rounded to 0 under retained four decimal places. According to the natural breakpoint method, the V_{reg_x} corresponding to all regionalization units can be divided into five levels or categories when *GVF* is greater than 0.7, as shown in Table 5. For example, if V_{reg_x} is larger than 0.1591, it belongs to level 5 with high vulnerability.

As can be seen from Fig. 11, the spatial distribution of the regionalization units with high, medium–high, and medium vulnerability is relatively clustered. In other words, the units with high vulnerability are mainly located in the Yangtze River Delta region, while the units with medium–high and medium vulnerability are mainly distributed in the east coastal regions of China. It is easy to find that the vulnerability level of the units located in the eastern regions is usually higher than that of other units. In particular, the vulnerability level of the units along the Beijing-Harbin, Chengdu-Chongqing, Beijing-Shanghai, and Zhengzhou-Xi'an lines is usually higher than that of other units. Furthermore, the units distributed in the urban agglomerations, such as the Beijing-Tianjin-Hebei, Chengdu-Chongqing, and central plains agglomerations, always belong to the high and medium–high vulnerability category. It reveals that the

Table 2
Failure situation and vulnerability of the HSRLN under different spaces of the typhoon.

Center	Influence scope	Number of failed lines	Number of failed trains	Vulnerability (0:00 ~ 24:00)
Hangzhou	100 km	5	786	0.2388
	200 km	10	1640	0.4064
Yancheng	100 km	5	362	0.1298
	200 km	8	954	0.2657
Qingdao	100 km	3	259	0.0706
	200 km	4	356	0.1012

Table 3
Vulnerability of the HSRLN under differently spatio-temporal scenarios of the typhoon.

Center	Influence scope	Influence time range		
		6:00 ~ 12:00	12:00 ~ 18:00	18:00 ~ 24:00
Hangzhou	100 km	0.1185	0.1889	0.1251
	200 km	0.2228	0.3297	0.2316
Yancheng	100 km	0.0612	0.1040	0.0736
	200 km	0.1461	0.2203	0.1533
Qingdao	100 km	0.0474	0.0665	0.0446
	200 km	0.0628	0.0925	0.0618

Table 4
Rank of top 10 critical HSR lines within the HSRLN under different periods.

Rank	All-day period		6:00 ~ 12:00		12:00 ~ 18:00		18:00 ~ 24:00	
	Critical lines	Vulnerability	Critical lines	Vulnerability	Critical lines	Vulnerability	Critical lines	Vulnerability
1	Beijing-Shanghai	0.3694	Beijing-Shanghai	0.2074	Beijing-Shanghai	0.3141	Beijing-Shanghai	0.2185
2	Shanghai-Kunming	0.2488	Shanghai-Kunming	0.1512	Shanghai-Kunming	0.2171	Shanghai-Kunming	0.1561
3	Shangqiu-Hangzhou	0.2076	Beijing-Guangzhou	0.1275	Shangqiu-Hangzhou	0.1831	Hangzhou-Shenzhen	0.1210
4	Hangzhou-Shenzhen	0.2072	Shangqiu-Hangzhou	0.1118	Hangzhou-Shenzhen	0.1637	Shangqiu-Hangzhou	0.1183
5	Beijing-Guangzhou	0.1801	Hangzhou-Shenzhen	0.1106	Beijing-Guangzhou	0.1610	Beijing-Guangzhou	0.1105
6	Nanjing-Chengdu	0.1567	Xuzhou-Lanzhou	0.1036	Nanjing-Chengdu	0.1424	Nanjing-Chengdu	0.1007
7	Beijing-Harbin	0.1490	Beijing-Harbin	0.0905	Xuzhou-Lanzhou	0.1271	Xuzhou-Lanzhou	0.1001
8	Xuzhou-Lanzhou	0.1399	Nanjing-Chengdu	0.0896	Beijing-Harbin	0.1264	Beijing-Harbin	0.0883
9	Nanjing-Hangzhou	0.0963	Tianjin-Tangshan	0.0562	Nanjing-Hangzhou	0.0868	Nanjing-Hangzhou	0.0571
10	Lianyungang-Zhenjiang	0.0875	Chengdu-Chongqing	0.0514	Hefei-Fuzhou	0.0722	Hefei-Fuzhou	0.0547

Table 5
Vulnerability classification of the HSRLN.

Level	Category	Standard
Level 1	Low vulnerability	$\leq$0.0171
Level 2	Medium-low vulnerability	0.0171 ~ 0.0416
Level 3	Medium vulnerability	0.0416 ~ 0.0796
Level 4	Medium-high vulnerability	0.0796 ~ 0.1591
Level 5	High vulnerability	>0.1591

disasters occurring in these regions can cause many lines and trains failure and can result in a great performance loss of the HSRLN. Nevertheless, the number of high and medium–high vulnerability units is significantly smaller than that of other category units as a whole.

5. Conclusions

This study investigates the vulnerability of HSRLN from a spatio-temporal perspective. First, a network model method is proposed to describe the HSRLN, in which an HSR line is first described as a sequential array of multiple HSR stations. The edges between the lines are established by the relations between the lines and HS trains. Next, the passenger volume and travel time cost are selected as the vulnerability indicators of HSRLN from the perspective of its function feature. Although the data of passenger volume is difficult to obtain, it can be estimated by its relation with the frequency and occupancy of HS trains. Furthermore, we develop a method for assessing the vulnerability of HSRLN based on its performance loss caused by disasters. In this study, a disaster is described from four dimensions, including its occurrence time and location, influence duration and scope. Then we propose a method for the identification of critical lines and the regionalization of vulnerability to protect HSRLN and reduce its performance loss. Finally, the HSRLN located in Mainland China is taken as the case study, and the obtained results can be summarized as follows.

Firstly, the HSRLN has the characteristic of a scale-free network in which the probability distribution of node degree follows to power law distribution. In the HSRLN, most of the lines are less connected to other lines, while a few lines are connected to many other

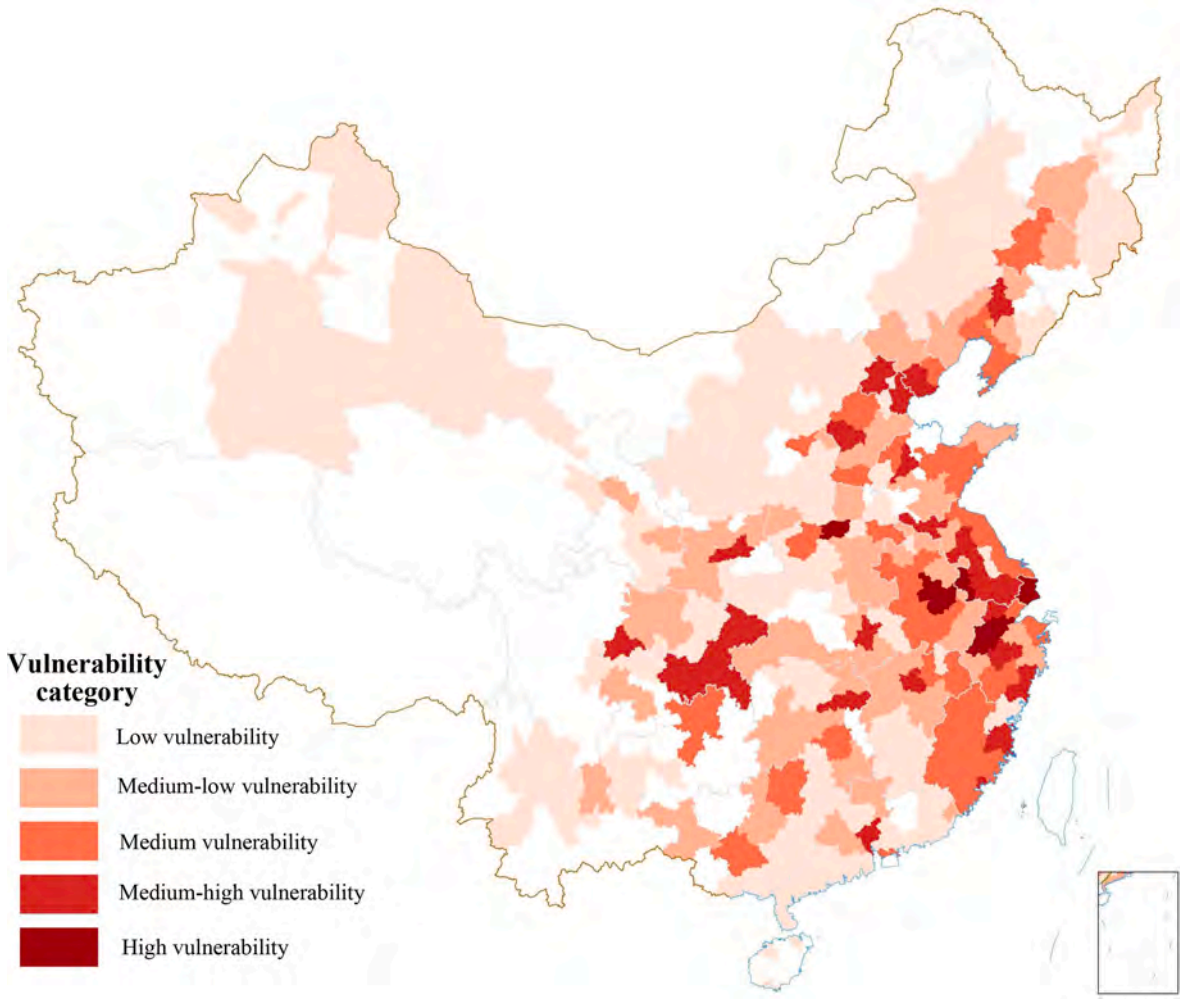

Fig. 11. Vulnerability regionalization map of the HSRLN.

lines. Moreover, the frequency of trains running on most of the lines is obviously smaller than that on a few lines. Therefore, the HSRLN is robust when suffering from the random failure of the lines or trains, while it is vulnerable under the malicious failure of the lines or trains.

Secondly, the disaster scenarios suffered by the HSRLN are very complex. The impact of a disaster on the HSRLN varies with its occurrence time and location, influence duration and scope. When the occurrence time and location, influence duration and scope of a disaster are different, the HSRLN can expose different vulnerabilities. For example, when the influence duration of a disaster is 6 h and 9 h, its occurrence at 11:00 can cause a larger vulnerability than that at other times. The disaster occurring in Hangzhou and Qingdao can result in the HSRLN's vulnerability to be equal to 0.1889 and 0.0665 respectively when its influence scope equals to 100 km and its influence time ranges from 12:00 to 18:00.

Thirdly, the criticality of different lines under different periods is different. A line failing at different times and different lines failing at the same time can make the HSRLN expose various vulnerabilities. For example, the failure of the Beijing-Guangzhou line during the period from 12:00 to 18:00 and from 18:00 to 24:00 can cause the HSRLN's vulnerability to be equal to 0.1610 and 0.1105 respectively. The failure of the Beijing-Guangzhou and Beijing-Harbin lines during the period from 6:00 to 12:00 can cause the vulnerability to be equal to 0.1275 and 0.0905 respectively.

Fourthly, different regions of Mainland China play different roles in the HSRLN's vulnerability. The regions with the high-level vulnerability of the HSRLN are mainly distributed in the Yangtze River Delta, while the regions with the medium–high-level and medium-level vulnerability are mainly located in the east coastal regions of China. The vulnerability level of the regions located in western China is usually lower than that of other regions.

Furthermore, some management implications can be obtained from the above findings. First, the administrators of HSR should recognize the unique characteristics and significance of HSRN from the HSR line perspective. The connections between HSR lines can exert critical impacts on the cascade failure within HSRLN. It is important to identify the difference of a new HSR line from others and its relation with others when planning or constructing it. Second, the spatio-temporal distinction of HSRLN's vulnerability should be

emphasized by administrators when developing the emergency planning of HSR. For example, the risk of the lines and trains failure occurring at 11:00 can be reduced, or even avoided by laying out more maintenance resources during this period. Third, more attention should be paid to the critical lines, essentially the lines ranked at the top in different periods, such as the Beijing-Shanghai, Shanghai-Kunming, Shangqiu-Hangzhou, and Beijing-Guangzhou lines within the HSRLN in Mainland China. Additionally, the layout of the maintenance resources for a line should focus on the critical time since the impact of its failure at the critical time on the vulnerability of HSRLN is larger than that at other times. At last, the regions with high-level vulnerability should be allocated more maintenance resources to monitor them. For example, the emergency rescue and resource reserve center of HSR can be set up to improve its capacity to respond to different disasters according to the vulnerability regionalization map.

However, many issues can be further explored from the limitations of this study. For the vulnerability evaluation, we do not account for the performance recovery under the disaster restoration measures when calculating the performance loss of HSRLN. If the data on the repair measures for the lines and trains after disasters is available, the performance recovery of HSRLN can be considered in future work. Although this work selects the passenger volume and travel time cost as the vulnerability metric from the function feature perspective of HSRLN, its vulnerability may involve multiple factors and dimensions, such as accessibility and size of the giant component (Sun et al., 2020a; Wandelt et al., 2024a). Therefore, more factors and dimensions can be taken into account from other perspectives in future studies. Nevertheless, the HSRLN is often described as an isolated network without consideration of its relations with other transportation networks. With the raid development of HSR, the relations between HSR lines and other transportation lines (such as airlines) are getting closer and closer (Xu et al., 2023b; Li et al., 2024), and therefore assessing the vulnerability of the comprehensive transportation network composed of HSR and other transportation with modal schedulings may be an interesting direction. Recently, the resilience of transportation networks, such as air and railway, has received increasing attention (Sun et al., 2020b; Ilalokhoin et al., 2023; Wandelt et al., 2024a, 2024b). Future works can investigate the resilience of HSRLN or HSRN. The case study and obtained results are limited to China. Other countries, such as Germany, also have developed HSR (Wandelt & Sun, 2022), which deserves to be investigated in the future as well.

CRediT authorship contribution statement

Tao Li: Writing – original draft, Software, Project administration, Methodology, Conceptualization. **Yu Qin:** Writing – original draft, Software, Methodology. **Mengqiao Xu:** Writing – review & editing, Validation, Data curation. **Yanjie Zhou:** Visualization, Validation, Software, Methodology, Investigation. **Lili Rong:** Supervision, Resources, Funding acquisition, Conceptualization.

Declaration of Competing Interest

The authors declare that they have no known competing financial interests or personal relationships that could have appeared to influence the work reported in this paper.

Data availability

Data will be made available on request.

Acknowledgements

This study is supported by Henan Philosophy and Social Science Program (grant no. 2023BJJ083), China Postdoctoral Science Foundation (grant no. 2023M733209), Key Research Programs of Higher Education Institutions in Henan Province (grant no. 24A630032), National Natural Science Foundation of China (grant no. 72201252 and 72271041). The authors would like to thank Prof. Anming Zhang (from Sauder School of Business, University of British Columbia), Dr. Anh Nguyentran (from University of California, Merced), and Peng Zhao (an engineer of China Railway) for their kind comments.

References

Albalate, D., Bel, G., 2012. High-speed rail: Lessons for policy makers from experiences abroad. Public Adm. Rev. 72 (3), 336–349.
Bugalia, N., Maemura, Y., Ozawa, K., 2020. Organizational and institutional factors affecting high-speed rail safety in Japan. Saf. Sci. 128, 104762.
Bugalia, N., Maemura, Y., Ozawa, K., 2021. Characteristics of enhanced safety coordination between high-speed rail operators and manufacturers. Reliab. Eng. Syst. Saf. 216, 107995.
Chen, Y.J., Chang, K.-H., Sheu, J.-B., Liu, C.-H., Chang, C.-C., Chang, C.-H., Wang, G.-X., 2023. Vulnerability-based regionalization for disaster management considering storms and earthquakes. Transp. Res. Part E: Logist. Transp. Rev. 169, 102987.
Chen, H., Jiang, B., 2019. A review of fault detection and diagnosis for the traction system in high-speed trains. IEEE Trans. Intell. Transp. Syst. 21 (2), 450–465.
Chen, Z., Wang, Y., 2019. Impacts of severe weather events on high-speed rail and aviation delays. Transp. Res. Part D: Transp. Environ. 69, 168–183.
Corman, F., D'Ariano, A., Hansen, I.A., 2014. Evaluating disturbance robustness of railway schedules. J. Intell. Transp. Syst. 18 (1), 106–120.
Deng, J., Liu, X., Jing, G., Bian, Z., 2018. Probabilistic risk analysis of flying ballast hazard on high-speed rail lines. Transp. Res. Part C: Emerg. Technol. 93, 396–409.
Feng, X., He, S., Li, G., Chi, J., 2021. Transfer network of high-speed rail and aviation: structure and critical components. Physica A 581, 126197.
Gao, Y., Liang, C., Zhou, J., Chen, S., 2023. Robustness optimization of aviation-high-speed rail coupling network. Physica A 610, 128406.
Gentile, G., Noekel, K., 2016. Modelling public transport passenger flows in the era of intelligent transport systems. Springer International Publishing, Gewerbestrasse.
Hong, W.-T., Clifton, G., Nelson, J.D., 2022. Rail transport system vulnerability analysis and policy implementation: past progress and future directions. Transp. Policy 128, 299–308.
Hong, L., Ye, B., Yan, H., Zhang, H., Ouyang, M., He, X.S., 2019. Spatiotemporal vulnerability analysis of railway systems with heterogeneous train flows. Transp. Res. A Policy Pract. 130, 725–744.

Hong, L., Ouyang, M., Xu, M., Hu, P., 2020. Time-varied accessibility and vulnerability analysis of integrated metro and high-speed rail systems. Reliab. Eng. Syst. Saf. 193, 106622.
Hu, Q., Bian, L., Tan, M., 2020. A data perception model for the safe operation of high-speed rail in rainstorms. Transp. Res. Part D: Transp. Environ. 83, 102326.
Hu, X., Huang, J., Shi, F., 2022. A robustness assessment with passenger flow data of high-speed rail network in China. Chaos Solitons Fractals 165, 112792.
Ilalokhoin, O., Pant, R., Hall, J.W., 2023. A model and methodology for resilience assessment of interdependent rail networks-case study of Great Britain's rail network. Reliab. Eng. Syst. Saf. 229, 108895.
Janić, M., 2018. Modelling the resilience of rail passenger transport networks affected by large-scale disruptive events: the case of HSR (high speed rail). Transportation 45, 1101–1137.
Jiao, J., Wang, J., Jin, F., 2017. Impacts of high-speed rail lines on the city network in China. J. Transp. Geogr. 60, 257–266.
Jiao, J., Zhang, F., Liu, J., 2020. A spatiotemporal analysis of the robustness of high-speed rail network in China. Transp. Res. Part D: Transp. Environ. 89, 102584.
Khademi, N., Babaei, M., Schmöcker, J.-D., Fani, A., 2018. Analysis of incident costs in a vulnerable sparse rail network-description and Iran case study. Res. Transp. Econ. 70, 9–27.
Khademi, N., Bababeik, M., Fani, A., 2021. Sparse rail network robustness analysis: functional vulnerability levels of accidents resulting from human errors. J. Safety Sci. Resilience 2 (3), 111–123.
Li, T., Rong, L., 2020. A comprehensive method for the robustness assessment of high-speed rail network with operation data: a case in China. Transp. Res. A Policy Pract. 132, 666–681.
Li, T., Rong, L., 2021. Impacts of service feature on vulnerability analysis of high-speed rail network. Transp. Policy 110, 238–253.
Li, T., Rong, L., 2022. Spatiotemporally complementary effect of high-speed rail network on robustness of aviation network. Transp. Res. A Policy Pract. 155, 95–114.
Li, T., Rong, L., Yan, K., 2019. Vulnerability analysis and critical area identification of public transport system: a case of high-speed rail and air transport coupling system in China. Transp. Res. A Policy Pract. 127, 55–70.
Li, T., Rong, L., Zhang, A., 2021. Assessing regional risk of COVID-19 infection from Wuhan via high-speed rail. Transp. Policy 106, 226–238.
Li, J., Sun, X., Cong, W., Miyoshi, C., Ying, L.C., Wandelt, S., 2024. On the air-HSR mode substitution in China: From the carbon intensity reduction perspective. Transp. Res. A Policy Pract. 180, 103977.
Mattsson, L.-G., Jenelius, E., 2015. Vulnerability and resilience of transport systems–a discussion of recent research. Transp. Res. A Policy Pract. 81, 16–34.
Nicholson, C.D., Barker, K., Ramirez-Marquez, J.E., 2016. Flow-based vulnerability measures for network component importance: experimentation with preparedness planning. Reliab. Eng. Syst. Saf. 145, 62–73.
Ouyang, M., Zhao, L., Hong, L., Pan, Z., 2014. Comparisons of complex network based models and real train flow model to analyze Chinese railway vulnerability. Reliab. Eng. Syst. Saf. 123, 38–46.
Ouyang, M., Pan, Z., Hong, L., He, Y., 2015. Vulnerability analysis of complementary transportation systems with applications to railway and airline systems in China. Reliab. Eng. Syst. Saf. 142, 248–257.
Ouyang, M., Tian, H., Wang, Z., Hong, L., Mao, Z., 2019. Critical infrastructure vulnerability to spatially localized failures with applications to Chinese railway system. Risk Anal. 39 (1), 180–194.
Read, G.J., Naweed, A., Salmon, P.M., 2019. Complexity on the rails: a systems-based approach to understanding safety management in rail transport. Reliab. Eng. Syst. Saf. 188, 352–365.
Reggiani, A., Nijkamp, P., Lanzi, D., 2015. Transport resilience and vulnerability: the role of connectivity. Transp. Res. A Policy Pract. 81, 4–15.
Rodríguez-Núñez, E., García-Palomares, J.C., 2014. Measuring the vulnerability of public transport networks. J. Transp. Geogr. 35, 50–63.
Sanchis, I.V., Franco, R.I., Fernández, P.M., Zuriaga, P.S., Torres, J.B.F., 2020. Risk of increasing temperature due to climate change on high-speed rail network in Spain. Transp. Res. Part D: Transp. Environ. 82, 102312.
Sun, X., Wandelt, S., Hansen, M., Li, A., 2017. Multiple airport regions based on inter-airport temporal distances. Transp. Res. Part E: Logist. Transp. Rev. 101, 84–98.
Sun, X., Wandelt, S., Hansen, M., 2020a. Airport road access at planet scale using population grid and openstreetmap. Netw. Spat. Econ. 20, 273–299.
Sun, X., Wandelt, S., Zhang, A., 2020b. Resilience of cities towards airport disruptions at global scale. Res. Transp. Bus. Manag. 34, 100452.
Sun, X., Wandelt, S., Zhang, A., 2021. Comparative accessibility of Chinese airports and high-speed railway stations: a high-resolution, yet scalable framework based on open data. J. Air Transp. Manag. 92, 102014.
URL. (2023). *High-speed around the world-Historical, geographical, and technological development.* International union of railways. https://uic.org/IMG/pdf/uic-high-speed-around-the_world.pdf.
Wandelt, S., Antoniou, C., Birolini, S., Delahaye, D., Dresner, M., Fu, X., Sun, X., 2024a. Status quo and challenges in air transport management research. J. Air Transp. Res. Soc. 2, 100014.
Wandelt, S., Sun, X., 2022. Lufthansa Express Rail in Germany: a critical evaluation of benefits and limitations of the intermodal network based on journey time and fares. Multimodal Transportation 1 (4), 100048.
Wandelt, S., Shi, X., Sun, X., 2021. Estimation and improvement of transportation network robustness by exploiting communities. Reliab. Eng. Syst. Saf. 206, 107307.
Wandelt, S., Sun, X., Zhang, A., 2023a. Towards analyzing the robustness of the Integrated Global Transportation Network Abstraction (IGTNA). Transp. Res. A Policy Pract. 178, 103838.
Wandelt, S., Xu, Y., Sun, X., 2023b. Measuring node importance in air transportation systems: on the quality of complex network estimations. Reliab. Eng. Syst. Saf. 240, 109596.
Wandelt, S., Sun, X., Zhang, J., 2024b. GraphCast for solving the air transportation nexus among safety, efficiency, and resilience. Commun. Transp. Res. 4, 100120.
Wang, L., 2019. Risk simulation analysis of high-speed rail disaster prevention system integration project based on GERT and Monte Carlo. Project Manag. Technol. 17 (01), 100–103.
Wang, Z., Chan, A.P., Yuan, J., Xia, B., Skitmore, M., Li, Q., 2015. Recent advances in modeling the vulnerability of transportation networks. J. Infrastruct. Syst. 21 (2), 06014002.
Wang, Z., Jia, L., Ma, X., Sun, X., Tang, Q., Qian, S., 2022. Accessibility-oriented performance evaluation of high-speed railways using a three-layer network model. Reliab. Eng. Syst. Saf. 222, 108411.
Wang, L., Liu, Y., Sun, C., Liu, Y., 2016. Accessibility impact of the present and future high-speed rail network: a case study of Jiangsu Province, China. J. Transp. Geogr. 54, 161–172.
Xu, M., Deng, W., Zhu, Y., Linyuan, L., 2023a. Assessing and improving the structural robustness of global liner shipping system: a motif-based network science approach. Reliab. Eng. Syst. Saf. 240, 109576.
Xu, M., Li, G., Chen, A., 2024. Resilience-driven post-disaster restoration of interdependent infrastructure systems under different decision-making environments. Reliab. Eng. Syst. Saf. 241, 109599.
Xu, Y., Wandelt, S., Sun, X., 2023b. IMMUNER: integrated multimodal mobility under network disruptions. IEEE Trans. Intell. Transp. Syst. 24 (2), 1480–1494.
Yang, H., Zhang, A., 2012. Effects of high-speed rail and air transport competition on prices, profits and welfare. Transp. Res. B Methodol. 46 (10), 1322–1333.
Yu, K., Strauss, J., Liu, S., Li, H., Kuang, X., Wu, J., 2021. Effects of railway speed on aviation demand and CO2 emissions in China. Transp. Res. Part D: Transp. Environ. 94, 102772.
Zhang, F., Graham, D.J., Wong, M.S.C., 2018a. Quantifying the substitutability and complementarity between high-speed rail and air transport. Transp. Res. A Policy Pract. 118, 191–215.
Zhang, J., Hu, F., Wang, S., Dai, Y., Wang, Y., 2016. Structural vulnerability and intervention of high speed railway networks. Physica A 462, 743–751.
Zhang, H., Ouyang, M., Sun, W., Hong, L., 2023. An approach for accessibility assessment and vulnerability analysis of national multimodal transport systems. Risk Anal. 43 (11), 2312–2329.
Zhang, Y., Zhang, A., 2016. Determinants of air passenger flows in China and gravity model: deregulation, LCCs, and high-speed rail. JTEP 50 (3), 287–303.
Zhang, Y., Lin, F., Zhang, A., 2018b. Gravity models in air transport research: a survey and an application. Handbook of International Trade and Transportation. Edward Elgar Publishing.